 DOI: 10.1002/masy.201050543

Scaling Behavior of Hyaluronic Acid in Solution with Mono- and Divalent Ions

E. Geissler,[*1] *A.-M. Hecht,*[1] *F. Horkay*[2]

Summry: The effect of the simultaneous presence of mono- and divalent cations on the thermodynamics of polyelectrolyte solutions is not fully understood. In physiological conditions, combinations of these ions affect structure formation in biopolymer systems. It is known that divalent counterions form a tight sheath around the polymer backbone, while monovalent ions are distributed in a diffuse cloud. Dynamic light scattering measurements of the collective diffusion coefficient D and the osmotic compressibility of semi-dilute hyaluronan solutions containing different ratios of sodium and calcium ions are compared with simple polyelectrolyte models. Scaling relationships are derived in terms of polymer concentration and ionic strength J of the added salt. Differences in the effects of sodium and calcium ions are expressed only through J.

Keywords: collective diffusion; dynamic light scattering; ion distribution; ionic strength; osmotic compression modulus; polyelectrolyte solutions

Introduction

Polyelectrolytes have acquired immense commercial interest over the past few decades. Even more importantly, and since a rather longer time, they occupy a central place in biological systems. Owing to the many length-scales that enter into the description of these polymers having ionizable groups, our understanding of their properties is less than complete. One of the main areas in which information is not systematically available,[1–4] or is simply lacking, relates to the presence of salt. Biopolymers in our body, for example, are exposed to physiological conditions in which both monovalent (sodium) and divalent (calcium) ions may simultaneously be present. These ions, along with others, play a pivotal role in biochemical reactions. It is known, for example, that addition of calcium ions can cause precipitation of gels composed of DNA.[5] Existing theories have little to say about the effects of multivalent ions, as they have focused on solutions containing only monovalent ions.[6,7] In highly charged systems with multivalent ions, the mean field Debye-Hückel and Poisson-Boltzmann models break down. More advanced physical models contain numerous assumptions and parameters, the experimental interpretation of which is not always straightforward. It is, therefore, timely to study the effects of ions of different valence on a well-defined polymer in near-physiological conditions, at concentrations not too far from those prevailing *in vivo*.

Here, we report systematic dynamic light scattering (DLS) observations of the effect of ions on the dynamics of semi-dilute solutions of a high molecular weight biopolymer, hyaluronan (HA), and compare the results with predictions of current theoretical models. HA, the sodium salt of hyaluronic acid, is one of the most abundant

[1] Laboratoire de Spectrométrie Physique CNRS UMR 5588, Université J. Fourier de Grenoble, BP 87, 38402 St Martin d'Hères cedex, France
Fax: (+33) 476 63 54 95;
E-mail: erik.geissler@ujf-grenoble.fr
[2] Section on Tissue Biophysics and Biomimetics, Program in Physical Biology, Eunice Kennedy Shriver National Institute of Child Health and Human Development, National Institutes of Health, 13 South Drive, Bethesda, MD 20892, USA

biopolymers in the body, being involved in the control of tissue hydration, in the rheology of synovial fluid, as well as in the self-assembly of proteoglycans in cartilage.[8] In all these functions, the osmotic response of the polymer is of paramount importance. The measurements reported here involve two physical quantities that contain osmotic information, namely the collective diffusion coefficient D of the solution and the DLS intensity R_θ. These were measured over a wide concentration range both of polymer and physiologically relevant ions (sodium and calcium). Results of measurements on this system using small-angle neutron scattering (SANS) and anomalous small-angle X-ray scattering (ASAXS) are also briefly discussed.

Experimental Part

The DLS measurements, using an ALV 5022F goniometer with a HeNe laser working at wavelength $\lambda = 6328$ Å, were made on aqueous solutions of HA ($M_w = 1.2 \times 10^6$ g mol^{-1}) at 50 and 100 mM NaCl and also in 100 mM NaCl with varying amounts of $CaCl_2$ (20, 50, 100, and 200 mM $CaCl_2$). The temperature was 25.0 ± 0.1 °C and the pH of the samples was 6.5, at which HA is completely dissociated.

SANS measurements were made on the NG3 instrument at the National Institute of Standards and Technology, Gaithersburg, Maryland, USA.[9] The range of wave vector q explored was $0.002\,\text{Å}^{-1} \leq q \leq 0.2\,\text{Å}^{-1}$. Counting times were from twenty minutes to two hours. D_2O was the solvent. After radial averaging, corrections for detector response and cell window scattering were applied. The neutron scattering intensities were calibrated using absolute intensity standards. All experiments were carried out at 25 ± 0.1 °C.

ASAXS measurements were made on the BM2 beam line at the European Synchrotron Radiation Facility, Grenoble, France. Corrections were made for dark current and distortion of the CCD camera. Measured intensities were normalized using a standard sample of known scattering cross-section. The transfer wave vector range explored was $0.008\,\text{Å}^{-1} \leq q \leq 1.0\,\text{Å}^{-1}$. To limit radiation damage effects, exposure times were limited to 20 s and the position of the beam in the sample was changed at each successive energy.

Results and Discussion

Figure 1 shows the SANS spectra of two solutions of HA at concentration 4% w/w, containing 0.1 M NaCl in D_2O. In this semi-dilute concentration range, unlike the dilute regime, chains from different molecules overlap strongly and the electrostatic interactions between them tend to create domains of partially ordered parallel arrays. At the low q end of Figure 1, power-law behavior with slope –3.2 dominates, characteristic of scattering from domain surfaces. At the high q end, power-law behavior also prevails, but the slope is close to –1, consistent with the extended linear form adopted by the polymer on this length scale. The remarkable feature of this figure is that addition of 0.1 M $CaCl_2$ to the solution is accompanied by only a minor increase in the scattering intensity. This increase is confined to the intermediate q region, which is governed by the thermodynamic concentration fluctuations.

The length-scale range in which mono- or divalent ions interact with the polymer backbone can be probed by ASAXS. Such measurements detect the change in scattering intensity that occurs when the incident X-ray energy is varied below the absorption edge E_a of the counterion. To bring E_a into a convenient energy range, the monovalent sodium ions were substituted by rubidium ions ($E_a = 15.199$ keV) and the divalent calcium ions by strontium ions ($E_a = 16.105$ keV). To illustrate the threshold effect, the variation with energy of the attenuation in a strontium chloride-containing solution of HA is shown in Figure 2. By measuring the difference in intensity in the scattering pattern far below the threshold and

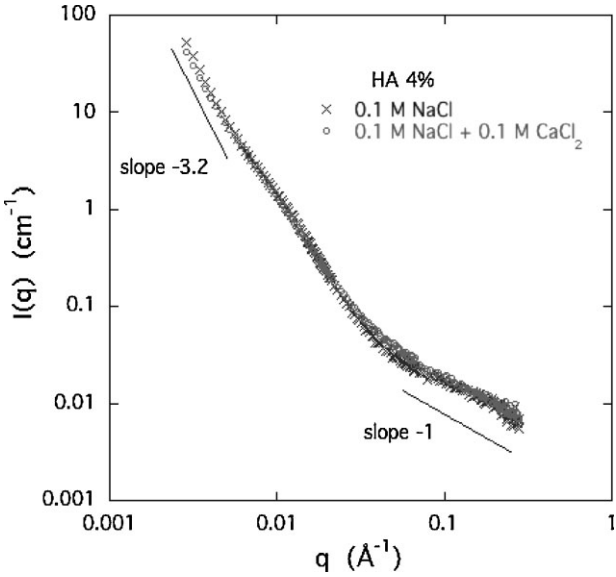

Figure 1.
SANS scattering response of a 4% w/w HA solution containing 0.1 M NaCl, with and without 0.1 M $CaCl_2$.

immediately below the threshold, the change in shape of the counterion cloud can be evaluated when monovalent ions are present alone and when they are accompanied by divalent ions (Figure 3). For the monovalent case, the agreement with a Poisson-Boltzmann distribution is good (dashed line). (Owing to the finite size of the polymer chain, however, uncertainty persists at small values of radial distance r). By contrast, the shape of the distribution of the Sr^{2+} ions is much more tightly

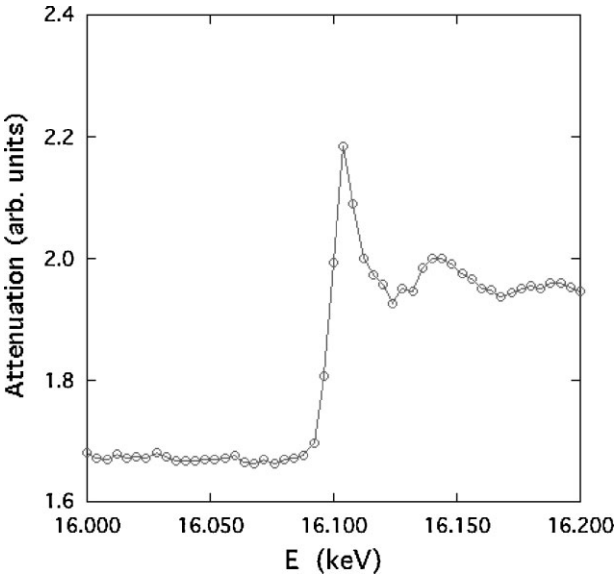

Figure 2.
Energy dependence of the transmitted intensity of the X-ray beam due to absorption in an HA solution containing 0.1 M NaCl and 0.1 M $SrCl_2$.

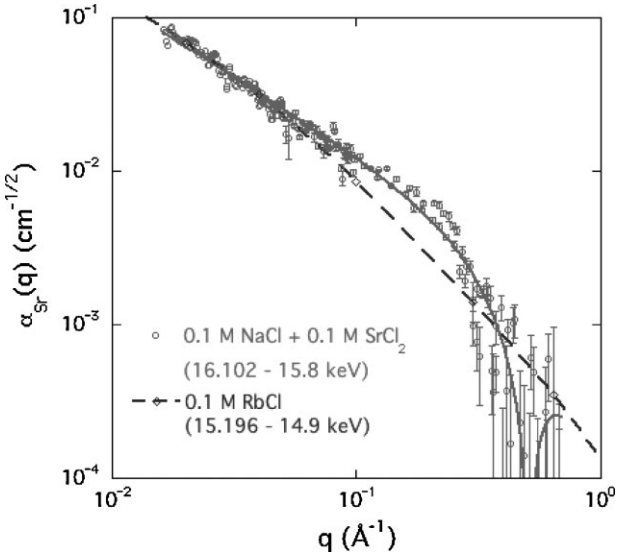

Figure 3.
Difference in scattering intensity between close to and far below the absorption threshold for HA solutions containing RbCl alone (dashed line) and 0.1 M NaCl with 0.1 M $SrCl_2$ (data points and continuous line). These data have been normalized with respect to the total scattered intensity.[10].

constrained, as demonstrated by the agreement of the data with the scattering curve of a solid cylinder (continuous line). Figure 4 illustrates the qualitative difference between these two distributions: unlike the monovalent ions, divalent ions are confined in a narrow sheath around the polymer backbone.[10] Since this sheath necessarily modifies the interaction of the polymer with the surrounding hydration layer, it might be reasonable to expect that the effect of counterion valence will substantially

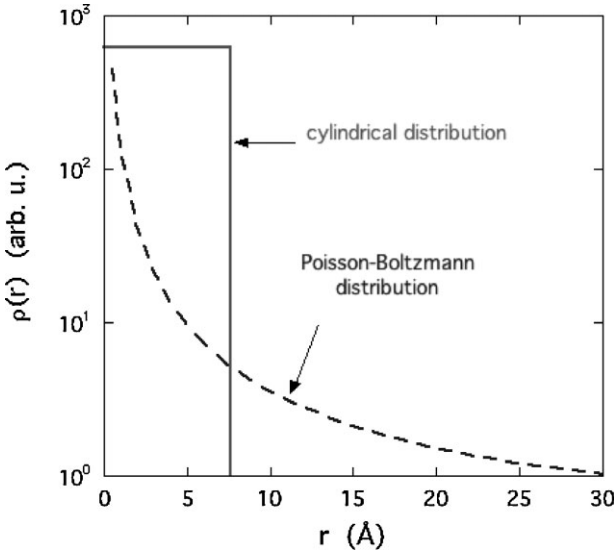

Figure 4.
Radial distribution density ρ(r) of the counterion cloud for Rb^{+} ions around a HA molecule (dashed curve) and for Sr^{2+} ions (continuous line).

influence the thermodynamics of the solution.

DLS probes the thermodynamics of a sample by measuring the amplitude and decay rate of the light $I(t)$ scattered by osmotic concentration fluctuations. Because these fluctuations are Gaussian, the intensity correlation function $g_2(\tau) = < I(t+\tau)I(t) > / < I(t) >^2$ of the scattered light is related to the field correlation function $g_1(\tau)$ by

$$g_2(\tau) = 1 + \beta|g_1(\tau)|^2 \quad (1)$$

where the angular brackets average over the experimental time and $\beta \approx 1$ is governed by the optics of the instrument. The light scattered by the HA solutions displays two components with different relaxation rates,

$$g_1(\tau) = a\exp(-\Gamma_f\tau) + (1-a)\exp[-(\Gamma_s\tau)^{\mu}] \quad (2)$$

in which the fast relaxation rate is governed by the collective diffusion coefficient D of the semidilute polymer solution

$$\Gamma_f = Dq^2 \quad (3)$$

As indicated in eq 2, the slow relaxation mechanism is described by a stretched exponential decay ($\mu \approx 2/3$, $\Gamma_s \propto q^3$) and is generated by internal modes of very large domains present in the solution. Owing to their size, these domains contribute negligibly to the osmotic pressure. The two relaxation components in the intensity correlation function are visible in the inset of Figure 5.

Figure 5 also shows how D varies with polymer concentration and also with salt content.[11] On increasing the salt concentration, especially with $CaCl_2$, D decreases. A natural way to present these data is in terms of the reduced variable c/J, where the ionic strength is $J = 1/2\ \Sigma c_i z_i^2$, z_i being the charge of the ith ion species, and where all the ion concentrations c_i are expressed in mol L^{-1}.

Figure 6 shows the resulting dependence of D on the reduced variable c/J. All

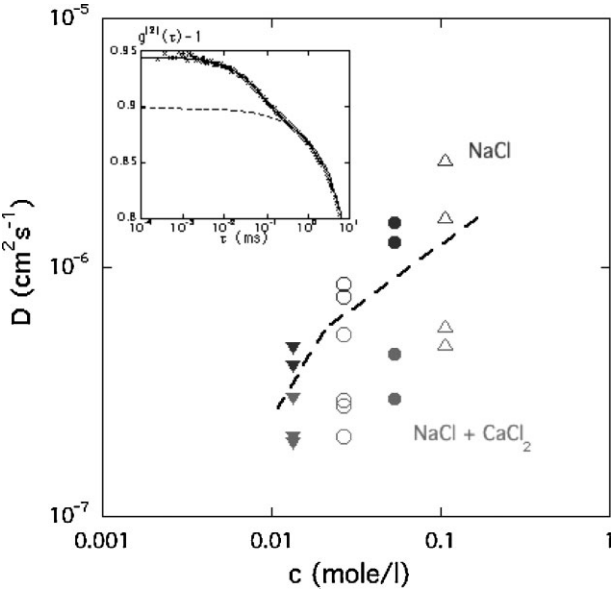

Figure 5.
Collective diffusion coefficient D at various polymer concentrations c. Increasing the salt concentration at fixed c decreases the value of D. Above the dashed line, the solution contains only NaCl; below the dashed line: 0.1 M NaCl with varying amounts of $CaCl_2$. Inset: fit of eq 2 to the intensity correlation function $g_2(\tau)$, showing the fast and slow components.

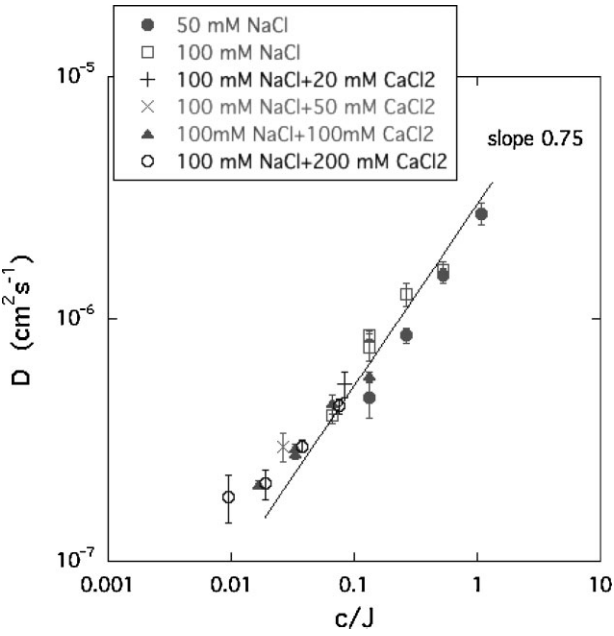

Figure 6.
Variation of *D* with c/*J*.

the data points fall on a plausible master curve that tends to a power-law at high values of c/J

$$D \propto (c/J)^{3/4} \tag{4}$$

Eq 4 captures the concentration dependence expected of a neutral polymer in excluded volume conditions.[12] The departure from this power-law behavior at low values of c/J is reminiscent of the approach to the dilute concentration regime, where D becomes independent of c. As will be seen from the behavior of the light scattering intensity, however, this similarity may be misleading.

The intensity of the scattered light, defined by the Rayleigh ratio $R_\theta = a < I(t) >$, is found from the decomposition of eq 2.[13,14] Its calibration is obtained using a standard sample (toluene). Because the spatial extent of the osmotic fluctuations (the correlation length ξ) is much smaller than $1/q$, R_θ is independent of the scattering angle θ. According to standard fluctuation theory, R_θ is inversely proportional to the osmotic modulus, $c\, d\Pi/dc$,

$$R_\theta = \left(\frac{2\pi n}{\lambda^2}\frac{dn}{dc}\right)^2 \frac{kTc^2}{(cd\Pi/dc)} \tag{5}$$

where Π is the osmotic pressure of the solution. In expression 5, dn/dc is the refractive index increment of the polymer-solvent pair, k is Boltzmann's constant and T is the absolute temperature. n is the refractive index of the index matching bath.[15]

To place the light scattering measurements in a theoretical framework, we recall that the osmotic properties of polymer solutions are determined by the correlation length ξ, which describes the mean distance between polymer segments. According to scaling theory, the osmotic pressure is proportional to the energy density of the concentration fluctuations, [12] i.e.,

$$\Pi \propto c\, d\Pi/dc \propto kT/\xi^3 \tag{6}$$

In the absence of added salt, a semidilute polyelectrolyte solution consists of domains in which linear segments of the polymers

form parallel arrays packed in such a way that the separation distance ξ between strands varies with concentration as $c^{-1/2}$. Neutralization with added salt is expected to create the conditions for a neutral polymer solution, i.e., $\xi \propto c^{-3/4}$. Cross-over between these limits can be achieved by setting $1/\xi \propto c^{1/2}/(1 + J/c)^{1/4}$.[7] At high salt content, this relation reduces to

$$1/\xi \propto c^{3/4}/J^{1/4} \tag{7}$$

and hence, by virtue of eq. 6, the osmotic compression modulus is

$$c\, d\Pi/dc \propto c^2/R_\theta \propto c^{9/4}/J^{3/4} \tag{8}$$

When the measured values of the quantity c^2/R_θ , which is proportional to the osmotic modulus, are plotted in a double-logarithmic representation as a function of the variable $c^{9/4}/J^{3/4}$ (Figure 7), they coalesce on an acceptable straight line with slope unity. This result, whereby the difference in valence between the two cations investigated exerts its influence on the thermodynamics of the solution only through the ionic strength J, is particularly striking in view of the qualitative difference in shape of the ion clouds. It is also notable that, even at the lowest values of $c^{9/4}/J^{3/4}$, the data display no sign of a change in slope that might be expected as the dilute concentration regime is approached.

The difference in scaling behavior between D and the intensity measurements suggests that there may be another length-scale at work. It is well known that the collective diffusion coefficient may be expressed as the ratio of the osmotic driving force $d\Pi/dc$ to the friction coefficient f between the polymer segments and the solvent, i.e., $D = (d\Pi/dc)/f$. It follows from eq 5 that the product

$$\frac{DR_\theta}{c} = \left(\frac{2\pi n}{\lambda^2}\frac{dn}{dc}\right)^2 \frac{kT}{f} \tag{9}$$

is independent of Π, and is a function only of the hydrodynamics of the polymer configuration. It is also notable that for neutral polymers in good solvent conditions, DR_θ/c varies as $c^{-1/2}$. In Figure 8, this same quantity, when plotted as a function of $c/J^{1/4}$, also exhibits power-law behavior,

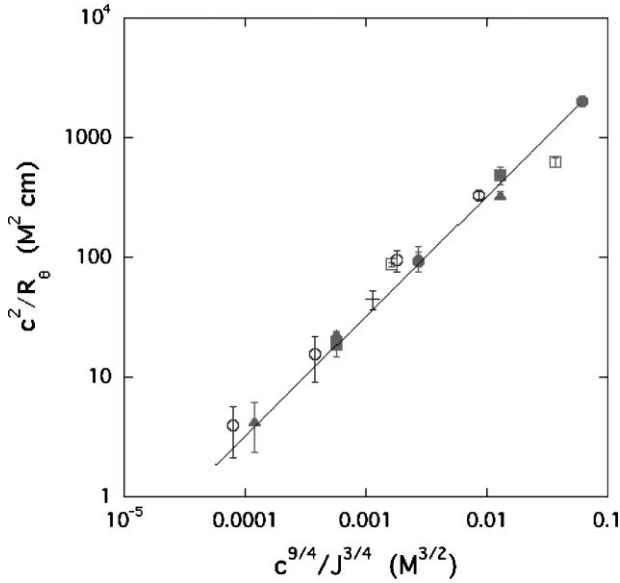

Figure 7.
Variation of c^2/R_θ, proportional to the osmotic modulus $c\, d\Pi/dc$, of HA solutions as a function of the variable $c^{9/4}/J^{3/4}$, where both c and J are expressed in mol L^{-1}. The slope of the straight line drawn through the data is 1. Symbols as in Figure 6.

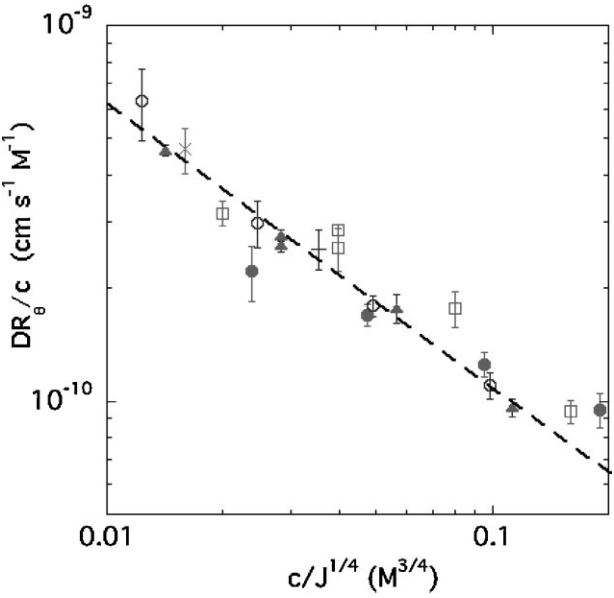

Figure 8.
Plot of DR_θ/c as a function of $c/J^{1/4}$. In this figure, small values of the friction coefficient f are found on the left-hand side, i.e., at high J, small c. The slope of the dashed line through the experimental points is −3/4.

revealing the existence of length-scale with a weak dependence on J. This finding suggests that the hydrodynamics of the segments in the semidilute solution is defined by the persistence length of the polymer: the friction coefficient f that is encountered, which is proportional to this length, decreases with increasing ionic strength.

Conclusion

This work reports measurements by dynamic light scattering of the diffusion coefficient D and the Rayleigh ratio R_θ of light scattered dynamically by concentration fluctuations in semi-dilute solutions of high molecular weight hyaluronan, containing both sodium chloride and calcium chloride in near physiological conditions. It is found that the osmotic modulus $c\ d\Pi/dc$ deduced from the measurements follows a simple scaling relationship of the form $c^{9/4}/J^{3/4}$, where c is the polymer concentration and J is the ionic strength of the added salt. In other words, under suitable conditions of neutralization, the solution behaves analogously to a neutral polymer in semi-dilute excluded volume conditions. The valence of the cation appears to affect the thermodynamics only through J. The ratio DR_θ/c, which depends only on hydrodynamic factors, displays a residual ionic strength dependence. It is conjectured that this effect is due to salt induced changes in the persistence length of the polymer in the semidilute state.

Acknowledgements: This research was supported by the Intramural Research Program of the NICHD, NIH, USA. The authors acknowledge the support of the National Institute of Standards and Technology, U.S. Department of Commerce for providing access to the NG3 small angle neutron scattering instrument and also to the European Synchrotron Radiation Facility for access to beam line BM2. The work utilized facilities supported in part by the National Science Foundation under Agreement No. DMR-0454672.

[1] S. Förster, M. Schmidt, M. Antonietti, *Polymer* **1990**, *31*, 781.
[2] M. Sedlak, E. J. Amis, *J. Chem. Phys.* **1992**, *96*, 817.
[3] J. J. Tanahatoe, M. E. Kuil, *J. Phys. Chem. B* **1997**, *101*, 9233.

[4] Y. Zhang, J. F. Douglas, B. D. Ermi, E. Amis, *J. Chem. Phys.* **2001**, *114*, 3299.
[5] F. Horkay, P. J. Basser, A.-M. Hecht, E. Geissler, *Macromol. Symp.* **2010**, this issue.
[6] T. Odijk, *Macromolecules* **1979**, *12*, 688.
[7] A. V. Dobrynin, M. Rubinstein, *Prog. Polym. Sci.* **2005**, *30*, 1049.
[8] S. Hokputsa, K. Jumel, C. Alexander, S. E. Harding, *Carbohydr. Polym.* **2003**, *52*, 111.
[9] NIST Cold Neutron Research Facility, NG3 and NG7 30-m. *SANS Instruments Data Acquisition Manual*, January **1999**.
[10] F. Horkay, A.-M. Hecht, C. Rochas, P. J. Basser, E. Geissler, *J. Chem. Phys.* **2006**, *125*, 234904.
[11] E. Geissler, A.-M. Hecht, F. Horkay, *Phys. Rev. Lett.* **2007**, *99*, 267801.
[12] P. G. de Gennes, *Scaling Concepts in Polymer Physics*, (Cornell University, Ithaca 1979).
[13] F. Horkay, W. Burchard, E. Geissler, A.-M. Hecht, *Macromolecules* **1993**, *26*, 1296.
[14] K. László, K. Kosik, E. Geissler, *Macromolecules* **2004**, *37*, 10067–10072.
[15] ALV-5000. *Multiple-tau Digital Correlator Reference Manual*, Langen, Germany 1993.

